MECHANICAL PROPERTIES ASSESSMENT FOR TPMS BASED SCAFFOLDS USING HOMOGENIZATION METHODS

J. PINHEIRO[1], A. P. G. CASTRO[1], R. B. RUBEN[2], J. M. GUEDES[1] AND P. R. FERNANDES[1]

[1]IDMEC, IST, University of Lisbon
Av. Rovisco Pais, 1049-001 Lisbon, Portugal
jp_juliapinheiro@hotmail.com; andre.castro@tecnico.ulisboa.pt; jmguedes@tecnico.ulisboa.pt;
paulo.rui.fernandes@tecnico.ulisboa.pt

[2]ESTG, CDRSP, Polytechnic Institute of Leiria
Campus 2 - Morro do Lena, Alto do Vieiro, 2411-901 Leiria, Portugal
rui.ruben@ipleiria.pt

Summary

The combination of computational methods with recent 3D printing technologies allows for the control of scaffolds microstructure, in order to obtain application-driven mechanical properties. Lately, geometries obtained using triply periodic minimal surfaces (TPMS) have been used to design porosity-controlled scaffolds for bone tissue engineering. The objective for this work is to assess the properties of TPMS scaffolds obtained using Schwartz P, Schwartz D and Gyroid, with different porosity levels. These properties are computed by an asymptotic homogenization method to obtain the effective permeability and stiffness. Results show that the obtained properties compare well with the properties of bone scaffolds presented in literature and obtained using different means.

1 INTRODUCTION

Scaffolds are porous structures that act as cellular support for the growth of new tissue [1]. For tissue engineering applications, scaffolds shall permit the diffusion of oxygen, nutrients and metabolic waste, in order to ensure adequate cellular growth and proliferation [2], [3]. In the specific case of bone tissue engineering, the structural integrity of the scaffolds is also important to enhance bone shape and function during and after the regeneration and remodelling processes [4]–[6]. Therefore, scaffolds must be optimized for appropriate porosity, permeability and mechanical properties [7].

Different techniques have been studied for the development of new application-driven scaffolds. This work is focused on the triply periodic minimal surfaces (TPMS) method. TPMS are defined mathematically as infinite and periodic surface curvatures that are fully controllable computationally and allow for homogenous scaffold designs [7]–[9]. This method targets scaffolds with a good relation between adequate levels of porosity and stiffness for different cellular growth rates [8], [10]–[12].

Apart from the development method, scaffolds shall be produced with enough accuracy, i.e.,

the designed structure shall correspond to the fabricated one. In the past, it has been found that produced scaffolds were different from the respective project [13], and this raised concerns about the applicability of these devices in the biomedical industry [13], [14]. Several technologies have been applied, as electrospinning or selective laser sintering, but this work is focused on 3D MultiJet printing. This is a good option for high accuracy scaffold production [15], [16].

2 METHODS

Three types of TPMS were selected (Schwartz D, Schwartz P and Gyroid), each one with two levels of porosity (50% and 70%). The selection of the porosities and surfaces was done based on the permeability since it is one of the main requirements for cellular growth and some geometries were not capable of having fluid through their interior and therefore could not be used. The TPMS were created with a custom software developed at the Polytechnic Institute of Leiria (Portugal) and CTI Renato Archer (Brazil) [17]. The asymptotic homogenization method described in Guedes and Kikuchi [18] allows the calculation of the equivalent elastic coefficients for periodic porous structures with the homogenised properties E_{ijkm}^H given by:

$$E_{ijkm}^H = \frac{1}{|Y|} \int_{\yen} E_{pqrs} \left(\delta_{rk}\delta_{sm} - \frac{\partial \bar{\chi}_r^{km}}{\partial y_s} \right) \left(\delta_{pi}\delta_{qj} - \frac{\partial \bar{\chi}_p^{ij}}{\partial y_q} \right) dY \qquad (1)$$

where $\bar{\chi}_r^{km}$ are the local deformation modes when the unit cell is subject to six unit average strains, E_{pqrs} are the elastic properties of the solid part ($\yen$) of the cell Y, $|Y|$ is the volume of the unit cell and δ_{ij} is the Kronecker delta. For this method, each single unit of the periodic scaffold was discretized with 20 finite elements per side.

Following the theoretical outputs, it is possible to evaluate the analogous mechanical properties in the printed scaffolds using specific testing equipment. The specimens created for mechanical testing were according to the ASTM norm D695 - 02a, which lead to parts with a height that was double of their width. One of the objectives here was to test the influence of the size of the unit cell side; the ideal dimensions from the norm were 12.7 x 12.7 x 25.4 mm and thus the closest values selected for the unit cell side were 2.5 mm and 3 mm. Since the work of Coelho et al. [19] stated that a minimum of five unit cells were necessary in each dimension, the final structures were built on 5x5x10 unit cells, in 2.5 mm and 3 mm side cells.

The parts were fabricated in a MJP 3600 3D printer from 3D Systems using multijet technology. The parts are printed in 3D Systems Crystal material and their technology uses a support material as well in order to allow the layer by layer construction with internal geometries. To have the final part the specimens go into a 3D Systems Product Finisher that provides the necessary heat to melt the support material and so remove it from the internal structures. All the Cleaning Procedures were done according to the supplier specifications. Figure 1 shows the finished parts.
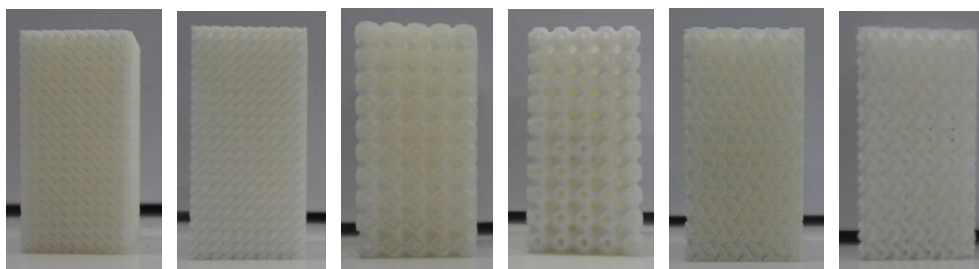
Figure 1: Printed specimens: D50, D70, P50, P70, G50 and G70.

Once the parts were printed they were mechanically tested in an Instron testing Machine 5566 equipped with an Advanced Video Extensometer (AVE), as can be seen in Figure 2. Mechanical tests were performed in order to obtain the elasticity properties (Young's Modulus) for the six scaffold types. The ASTM norm D695 - 02a was followed and therefore seven specimens were tested for each geometry (more than the five specimens specified as the minimum by the norm), being the testing speed set to 1.3 mm/min.
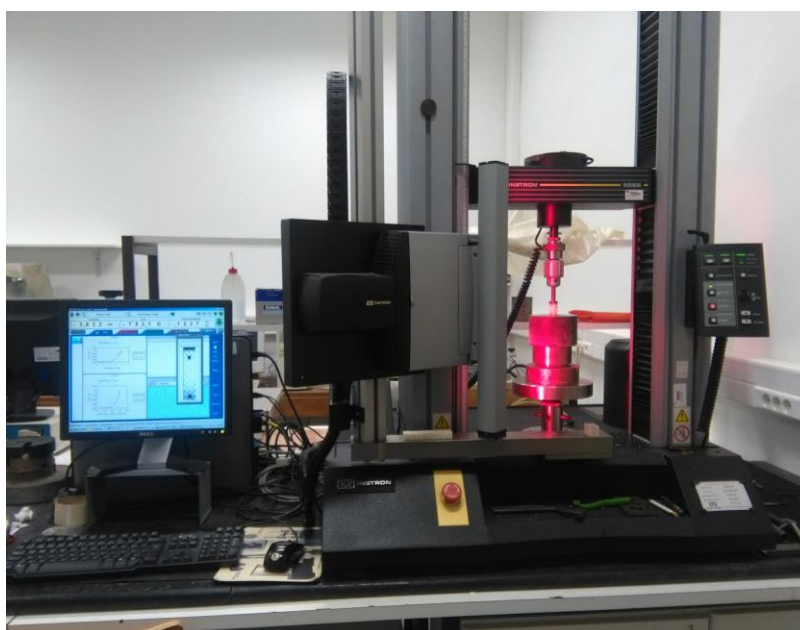
Figure 2: Setup of the experimental testing using an Instron 5566 and an Instron AVE.

3 RESULTS

Young's Modulus values were calculated from both experiments and numerical methods. Thus, Tables 1 (2.5mm unit cell side) and 2 (3mm unit cell side) present the values from the testing machine arm ("ARM"), from the video extensometer ("AVE") and from the

homogenization method ("HMG"). The standard deviation values from each experimental method are also presented ("std"). The last two columns of each table present the difference (error) between the experimental method and the theoretical results ("Error HMG-ARM" and "Error HMG-AVE"). Additionally, Figure 3 shows different failure modes for the same scaffold type obtained during the mechanical testing.

Table 1: Experimental and numerical Young's Modulus values (in MPa) for 2.5mm unit cell side.

Model	ARM	std	AVE	std	HMG	Error HMG-ARM	Error HMG-AVE
D50	0.3410	0.0337	0.4013	0.0251	0.2655	0.28	0.51
D70	0.1007	0.0165	0.1098	0.0244	0.1338	0.25	0.18
P50	0.3000	0.0067	0.3188	0.1255	0.2434	0.23	0.31
P70	0.0798	0.0018	0.0893	0.0070	0.0852	0.06	0.05
G50	0.2485	0.0068	0.2731	0.0123	0.2296	0.08	0.19
G70	0.1005	0.0035	0.1086	0.0029	0.1070	0.06	0.01

Table 2: Experimental and numerical Young Modulus values (in MPa) for 3mm unit cell side.

Model	ARM	std	AVE	std	HMG	Error HMG-ARM	Error HMG-AVE
D50	0.2509	0.0093	0.2872	0.0171	0.2655	0.05	0.08
D70	0.1026	0.0025	0.1164	0.0069	0.1338	0.23	0.13
P50	0.2592	0.0093	0.2740	0.1151	0.2434	0.06	0.13
P70	0.0821	0.0034	0.0954	0.0049	0.0852	0.04	0.12
G50	0.2258	0.0084	0.2622	0.0110	0.2296	0.02	0.14
G70	0.2509	0.0093	0.2872	0.0171	0.2655	0.05	0.08
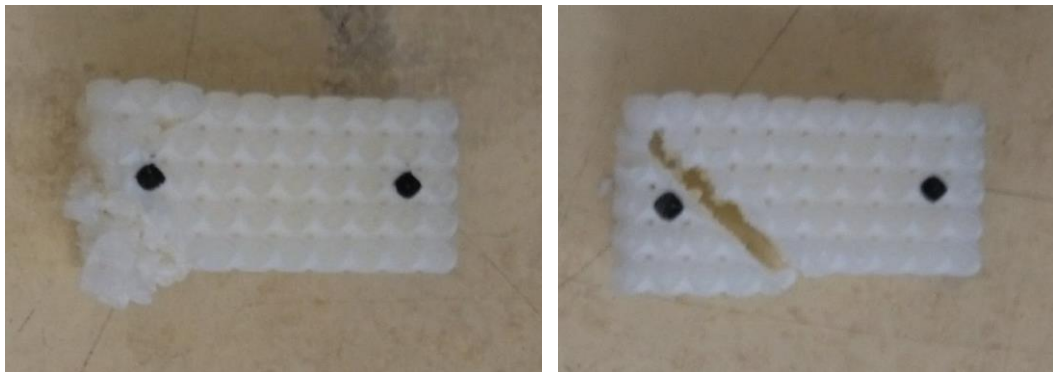
Figure 3: Different failure modes of specimens of the same type during mechanical testing.

4 DISCUSSION

As was already reported by other works in the literature [7], [9], [10], [12], Schwartz D is the one with the highest values of elasticity, for each porosity level, in comparison with Schwartz P and Gyroid. Only two levels of porosity were studied, which may not be enough to conclude about the stiffness differences between TPMS surfaces. However, it is relevant to emphasize the role of numerical studies in organizing information and comparing different printed TPMS scaffold types with different porosities. The Young's Modulus for the different porosities were according to what was theoretically expected, having higher values for lower porosities. Here again, further tests should be performed, with other TPMS scaffold types and potentially other porosity levels, in order to allow for the development of a trendline for each surface according to its porosity.

Regarding the difference between the unit cell side size, from 2.5mm to 3mm, it seems that this type of technology presents some difficulties for very small pore sizes, as the support material is hard to remove. Although the precision of the printer used is around 16μm, which is reflected in a great accuracy in the physical representation of the designed part, the cleaning postprocessing is manual and is most likely be not efficient enough.

Some works in the literature reported the mechanical structures of several TPMS surfaces and different porosities. For example, it is possible to compare this work with the one from Kapfer et al. [20], although the geometries tested were only of 50% of porosity. For Schwartz P the result was 0.226 MPa, for Schwartz D 0.232 MPa and for Gyroid 0.233 MPa. The results were similar to the ones here obtained, particularly for the Gyroid geometries.

The failure modes, as shown in Figure 3, were diverse (some specimens were destroyed during the testing and therefore no photographs could be taken) and were according to results also reported in the literature [7].

Some factors need to be considered to explain the errors present in Tables 1 and 2. The differences in the measurements from the ARM and the AVE were significant and it is possible to see that the results from ARM are closed to the theoretical values. The AVE is not recommended for compression tests especially with specimens smaller than 50 mm, according to the instructions of the manufacturer. This may partially justify the larger error seen in the AVE results.

It is also possible to observe a higher error in the smaller geometries (with 2.5 mm of side). This can probably be explained by the issues found the removal of the support material from the printing technology. This means that due to the viscosity of this wax (recommended by the printer manufacturer) it was difficult to remove the support material through the small pores of the geometries. Therefore, the larger parts (with 3mm of side) were "cleaner" and the results are noticeably better. The presence of support material inside the parts, particularly the ones with smaller pores (as is the case of the Schwartz D geometry) are not reflecting the real elastic properties of the material, but the properties of the material plus the residual wax.

5 CONCLUSIONS

This work allowed a good comparison between three of the most used TPMS structures for different porosities. Schwartz D is the surface with higher elasticity modulus, which means that for scaffolds with higher need for strength it should be the one more capable.

There are several groups working on the relation between permeability and elasticity in these scaffolds, as they need to be carefully designed to account for both paraments. Permeability and elasticity are essential to promote appropriate cellular growth and proliferation, and this work is helping to expand the knowledge base in this area.

To conclude, it was possible to assess that for this type of fabrication the design process should provide large enough pores to allow for the removal of the support material used during the printing process, as this material has a high viscosity, which hinders its removal from very delicate microstructures. Subsequently, for the larger structures studied here, this technology allows for good agreement with theoretical predictions.

6 ACKNOLEDGEMENTS

7 REFERENCES

[1]   A. Boccaccio, "Finite Element Method (FEM), Mechanobiology and Biomimetic Scaffolds in Bone Tissue Engineering," *Int. J. Biol. Sci.*, vol. 7, no. 1, pp. 112–132, 2011.

[2]   A. L. Olivares and D. Lacroix, "Simulation of cell seeding within a three-dimensional porous scaffold: a fluid-particle analysis.," *Tissue Eng. Part C. Methods*, vol. 18, no. 8, pp. 624–31, 2012.

[3]   A. Rahbari, H. Montazerian, E. Davoodi, and S. Homayoonfar, "Predicting permeability of regular tissue engineering scaffolds: scaling analysis of pore architecture, scaffold length, and fluid flow rate effects," *Comput. Methods Biomech. Biomed. Engin.*, vol. 5842, no. August, pp. 1–11, 2016.

[4]   I. Papantoniou *et al.*, "Spatial optimization in perfusion bioreactors improves bone tissue-engineered construct quality attributes," *Biotechnol. Bioeng.*, vol. 111, no. 12, pp. 2560–2570, 2014.

[5]   H. C. Rodrigues, P. G. Coelho, and P. R. Fernandes, "Multiscale modelling of bone tissue - Remodelling and application to scaffold design," *Comput. Methods Appl. Sci.*, vol. 20, pp. 15–33, 2011.

[6]   G. D. G. Barabaschi and V. Manoharan, "Engineering Mineralized and Load Bearing Tissues," *Adv. Exp. Med. Biol.*, vol. 881, pp. 79–94, 2015.

[7]   F. S. L. Bobbert *et al.*, "Additively manufactured metallic porous biomaterials based on minimal surfaces: A unique combination of topological, mechanical, and mass transport properties," *Acta Biomater.*, vol. 53, pp. 572–584, 2017.

[8]   R. Gauvin *et al.*, "Microfabrication of complex porous tissue engineering scaffolds using 3D projection stereolithography," *Biomaterials*, vol. 33, no. 15, pp. 3824–3834, May 2012.

[9]   H. Montazerian, E. Davoodi, M. Asadi-Eydivand, J. Kadkhodapour, and M. Solati-Hashjin, "Porous scaffold internal architecture design based on minimal surfaces: A compromise between permeability and elastic properties," *Mater. Des.*, vol. 126, no.

April, pp. 98–114, 2017.

[10] S. B. G. Blanquer *et al.*, "Surface curvature in triply-periodic minimal surface architectures as a distinct design parameter in preparing advanced tissue engineering scaffolds," *Biofabrication*, vol. 9, no. 2, 2017.

[11] S. M. Giannitelli, D. Accoto, M. Trombetta, and A. Rainer, "Current trends in the design of scaffolds for computer-aided tissue engineering," *Acta Biomater.*, vol. 10, no. 2, pp. 580–594, 2014.

[12] S. Rajagopalan and R. A. Robb, "Schwarz meets Schwann: Design and fabrication of biomorphic and durataxic tissue engineering scaffolds," *Med. Image Anal.*, vol. 10, no. 5, pp. 693–712, 2006.

[13] A. Campos Marin and D. Lacroix, "The inter-sample structural variability of regular tissue-engineered scaffolds significantly affects the micromechanical local cell environment," *Interface Focus*, vol. 5, no. 2, pp. 20140097–20140097, 2015.

[14] A. P. G. Castro and D. Lacroix, "Micromechanical study of the load transfer in a polycaprolactone–collagen hybrid scaffold when subjected to unconfined and confined compression," *Biomech. Model. Mechanobiol.*, Nov. 2017.

[15] M. Castilho, I. Pires, B. Gouveia, and J. Rodrigues, "Structural evaluation of scaffolds prototypes produced by three-dimensional printing," *Int. J. Adv. Manuf. Technol.*, vol. 56, no. 5–8, pp. 561–569, 2011.

[16] S. J. Hollister *et al.*, "Design Control for Clinical Translation of 3D Printed Modular Scaffolds," *Ann. Biomed. Eng.*, vol. 43, no. 3, pp. 774–786, 2015.

[17] J. C. Dinis *et al.*, "Open Source Software for the Automatic Design of Scaffold Structures for Tissue Engineering Applications," *Procedia Technol.*, vol. 16, pp. 1542–1547, 2014.

[18] J. M. Guedes and N. Kikuchi, "Preprocessing and postprocessing for materials based on the homogenization method with adaptive finite element methods," *Comput. Methods Appl. Mech. Eng.*, vol. 83, no. 2, pp. 143–198, Oct. 1990.

[19] P. G. Coelho, S. J. Hollister, C. L. Flanagan, and P. R. Fernandes, "Bioresorbable scaffolds for bone tissue engineering: Optimal design, fabrication, mechanical testing and scale-size effects analysis," *Med. Eng. Phys.*, vol. 37, no. 3, pp. 287–296, 2015.

[20] S. C. Kapfer, S. T. Hyde, K. Mecke, C. H. Arns, and G. E. Schröder-Turk, "Minimal surface scaffold designs for tissue engineering," *Biomaterials*, vol. 32, no. 29, pp. 6875–6882, 2011.